Crystal Growth in Liquid Steel during Secondary Metallurgy

R. DEKKERS, B. BLANPAIN, and P. WOLLANTS

Morphology of nonmetallic inclusions depends on their crystallographic structure, the growth conditions, and the presence of impurities. Inclusions were extracted from industrial aluminum-killed steel samples and investigated under high-resolution scanning electron microscopy. In this article, the morphology of these aluminum oxide inclusions, including their surface features, is approached from the viewpoint of crystal growth. Commonly, aluminum oxide inclusions are considered to be corundum, but some inclusion shapes prove that other aluminum oxide polymorphs are present as well.

I. INTRODUCTION

IN aluminum-killed steel, inclusions show a variety of morphologies. Globular iron aluminates, which can be enveloped by aluminum oxide, and pure aluminum oxide inclusions, which may occur as spheres, polyhedra, plates, dendrites, and clusters, have been described.[1–12] In particular, Steinmetz *et al.*[4–6,11,12] were aware that the morphology of an inclusion depends not only on its phase, but also on the activities of its components in the steel bath, *i.e.*, on the degree of supersaturation. They studied the relationship between inclusion morphology and the aluminum and oxygen contents of the steel. Their experiments concerned both deoxidation and reoxidation. In summary, they observed that, in order of decreasing oxygen content, globular iron aluminates, dendrites, and finally polyhedra are formed. Clusters (coral-shaped) of aluminum oxide particles are formed at the interface between oxygen-rich steel and deoxidized steel.

Over the past decade, research on the relationship between the morphology of aluminum oxide inclusions and the conditions in the ladle seems to have dwindled, while both steelmaking practice and steel chemistry have changed considerably. The oxygen contents reported in the aforementioned articles are higher than those of modern steelmaking. As a result, iron aluminates are not observed anymore and dendrites are observed only occasionally. Furthermore, devices for liquid steel sampling have been developed, which enable investigation of steel cleanliness during secondary metallurgy.

In a preceding article,[13] we showed what inclusions are present in the liquid steel and how these inclusions evolve during ladle metallurgy at Sidmar. Steel grades investigated were low-carbon aluminum-killed (LCAK), medium-carbon aluminum-killed (MCAK) and low-carbon silicon-aluminum killed grades (LCSAK). The composition ranges of the steels are listed in Table I. Samples of the liquid steel were taken automatically with short time intervals (1 to 2 minutes) by using the total oxygen sampling (TOS, Heraeus Electro-Nite) system. The small diameter of a TOS sample (4 mm) ensures fast cooling, and argon flushing inhibits reoxidation of the steel during sampling. Inclusions were extracted by dissolving the steel matrix in hot hydrochloric acid.[14,15] The solution with inclusions was filtered by using a Nuclepore membrane with pores of 0.2 μm. Next, the membrane with inclusions was coated with carbon and investigated by using scanning electron microscopy (PHILIPS* XL30 FEG). The extraction method is inappropriate for sulfides, silicates ($MnSiO_3$ was detected in a polished sample), and some nitrides, *e.g.*, AlN. Chemical analysis was carried out by energy dispersive spectrometry. Spherical manganese silicate ($MnSiO_3$) inclusions were observed after silicon addition and before aluminum addition. After deoxidation with aluminum, only aluminum oxide inclusions have been observed. Small faceted and platelike particles contained frequently magnesium, up to 4 at. pct.

*PHILIPS is a trademark of Philips Electronic Instruments Corp., Mahwah, NJ.

The ladle treatment at Sidmar starts with tapping of the converter, a basic oxygen furnace, holding 300 tons of steel at about 1923 K. During tapping, alloying elements and deoxidation elements can be added, *e.g.*, carbon, manganese, silicon, and aluminum. Then, the slag, consisting of entrapped converter slag and deoxidation products, is skimmed and replaced by a synthetic slag that consists mainly of calcium oxide and, dependent on the steel composition, bauxite. Subsequently, aluminum lumps are added. The steel composition is finally adjusted by appropriate alloying. During deoxidation and alloying, the steel is stirred by argon or by nitrogen, commonly for 10 to 30 minutes. The secondary metallurgy treatment, from tapping until casting, takes about 95 minutes.

In the present article, morphologies of inclusions are explained by considering steel conditions during their formation and growth. The steel grade (Table I) and the time of sampling elapsed after deoxidation (aluminum addition) are listed between brackets in the caption of every micrograph. The steel temperature was about 1873 K. High-resolution scanning electron microscopy reveals surface features, which can be understood by considering crystal growth mechanisms.

II. CRYSTAL GROWTH

The morphology of inclusions as observed under the microscope is the accumulative result of the growth (or dissolution) conditions the particle encounters from the

R. DEKKERS, Scientific Researcher, B. BLANPAIN, Associate Professor, and P. WOLLANTS, Full Professor, are with the Department of Metallurgy and Materials Engineering, Katholieke Universiteit Leuven, B-3001 Heverlee (Leuven), Belgium. Contact e-mail: Rob.Dekkers@mtm.kuleuven.ac.be

Manuscript submitted November 26, 2001.

Table I. Compositional Ranges in Parts per Million of the Investigated Steel Grades

Element	MCAK	LCSAK	LCAK
C	1100 to 1400	0 to 450	250 to 450
Mn	5500 to 6000	6200 to 7700	1500 to 2300
Si	0 to 200	2000 to 2600	0 to 200
P	0 to 180	0 to 200	0 to 120
Al	150 to 550	150 to 300	300 to 650

Fig. 1—Microscopic surface topology in the case of BCF-controlled growth (left) and VKS-controlled growth (right) (adapted from Ref. 17.)

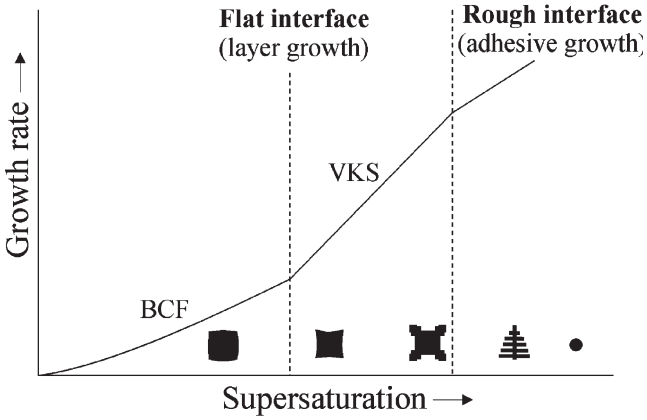

Fig. 2—Schematic diagram showing the relationship between supersaturation and the growth rate for BCF, VKS, and adhesive growth (adapted from Ref. 17.)

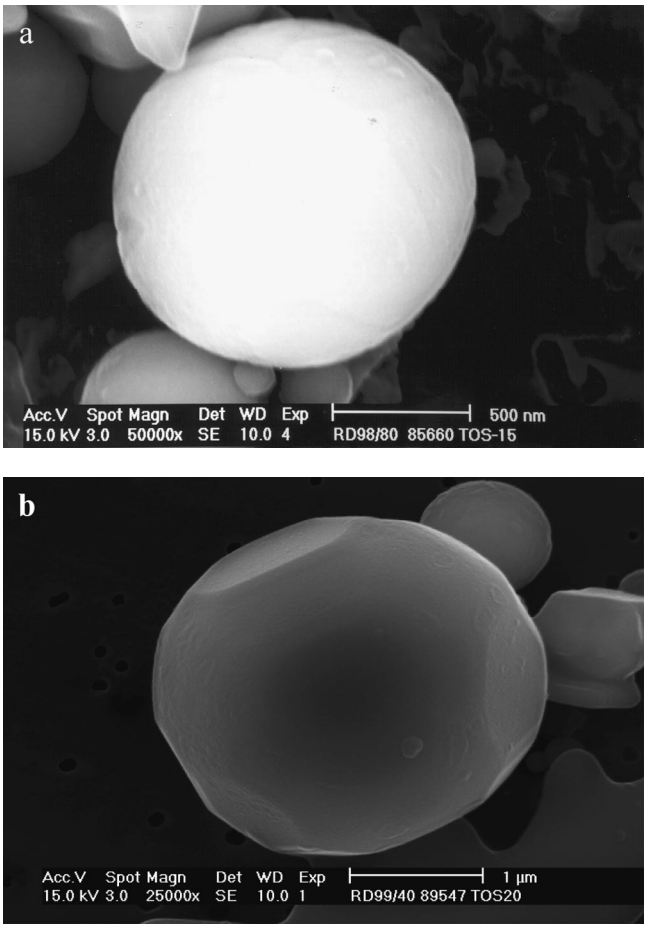

Fig. 3—Spherical aluminum oxide particles ((*a*) MCAK–19′44″) may develop facets ((*b*) LCSAK–36′25″) as the supersaturation decreases.

moment of its formation until the moment of sampling (provided that the sampling and the preparation technique do not affect the inclusions).

Crystal growth is a dynamic process during which the number of attaching units is larger than the number of detaching (dissolving) units. The attaching units can be atoms, molecules, or complexes. Crystal growth is driven by the difference in Gibbs free energy. Its mechanism depends largely on the ability to arrange the flux of attaching growth units on the crystal surface (at this point, agglomeration and clustering are not considered).

Crystals tend to grow with facets, because this maximizes bond formation within a growth slice and therefore minimizes surface energy. The law of Bravais–Friedel–Donnay–Harker correlates the occurrence of facets on a crystal with its three-dimensional atomic arrangement. Taking into account the effect of screw axes and glide planes, the minimum spacing between equivalent surfaces, d_{hkl}, is related to the importance of that face on the crystal habit.[16]

Apart from the crystal structure, morphology also depends on the roughness of the crystal surface. On an atomic scale, the surface can be either flat or rough. Facets are flat surfaces and two mechanisms of growth are recognized, *i.e.*, two-dimensional nucleation and spiral growth. The Volmer–Kossel–Stranski (VKS) model[17] considers the formation of a two-dimensional nucleus onto a flat surface. Once a stable nucleus is formed, steps at its boundaries are preferred sites for attachment of growth units and the new layer quickly spreads over the surface. A new two-dimensional nucleus is required for the formation of the next layer. Therefore, the growth rate depends on the nucleation rate, which depends on the levels of supersaturation. With respect to the formation of aluminum oxide, supersaturation (σ) can be defined as

$$\sigma = \frac{-RT \ln (a_{\underline{O}}^3 \cdot a_{\underline{Al}}^2) + \Delta G^{\circ}_{Al_2O_3}}{\Delta G^{\circ}_{Al_2O_3}} \qquad [1]$$

where $a_{\underline{O}}$ and $a_{\underline{Al}}$ refer to the activity of oxygen and the activity of aluminum in the steel bath. The term $\Delta G^{\circ}_{Al_2O_3}$ is the standard formation free energy of aluminum oxide, R is the gas constant, and T is the absolute temperature. Burton–Cabrera–Frank (BCF) explained that crystal growth may even occur at very low supersaturation.[17] They considered that outcropping screw dislocations creates a continuous step at the crystal surface. In this case, nucleation is not necessary and the growth rate is related to the dimensions of the screw dislocation (distance between its steps) and residence time of an attaching growth unit on the crystals surface.

If the supply of attaching growth units on the crystal surface exceeds the number that can be accommodated by the BCF or the VKS mechanism, the morphology changes

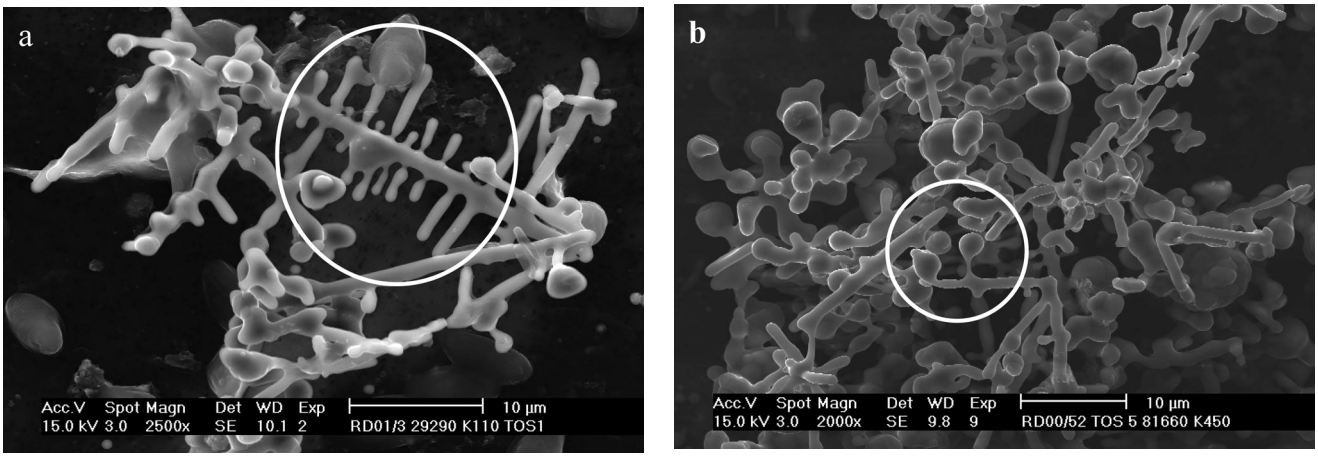

Fig. 4—Coarsening of dendritic clusters (within white circles) ((*a*) LCAK–5′ and (*b*) MCAK–7′38″).

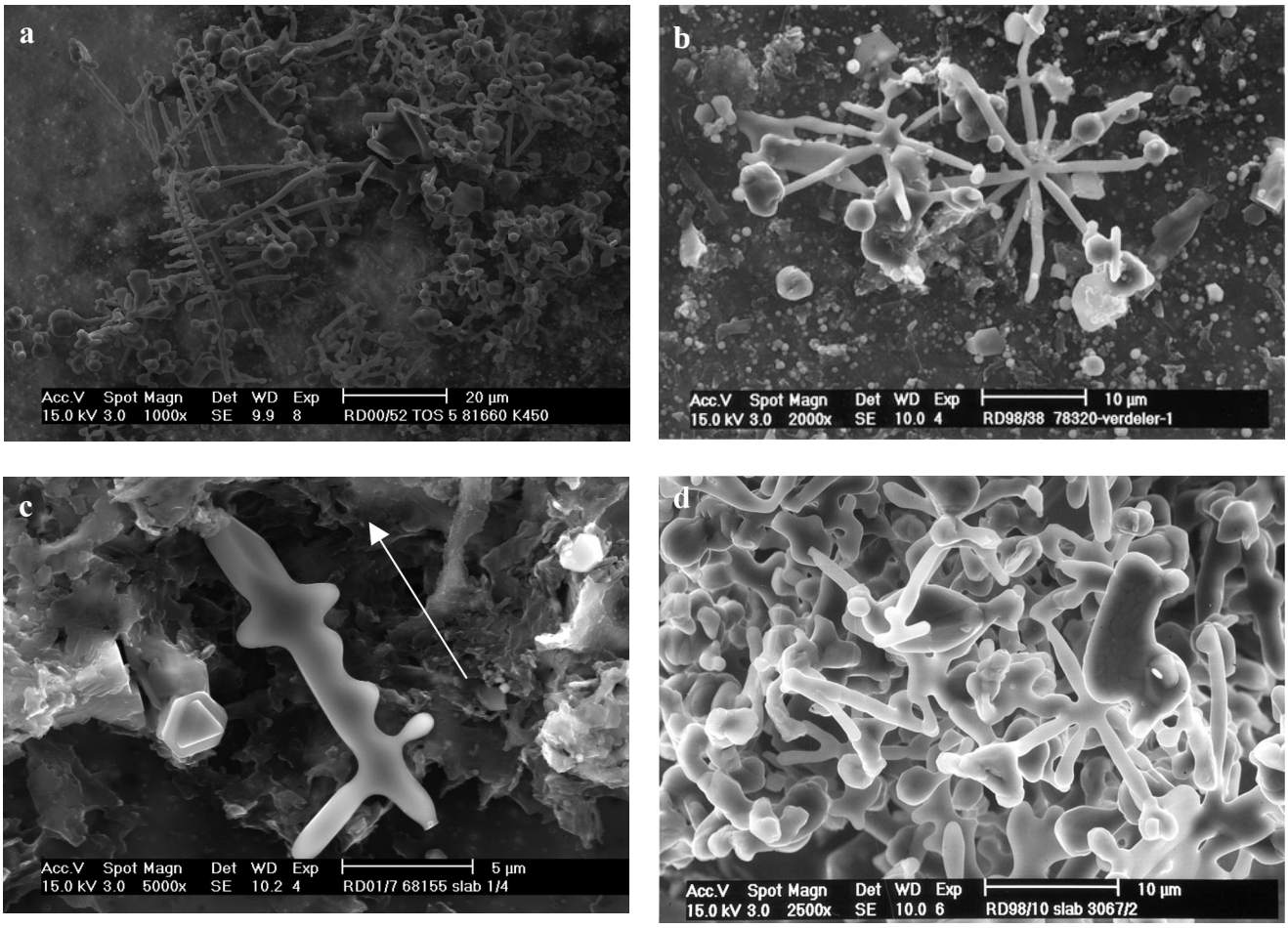

Fig. 5—Dendritic clusters in ladle (*a*) MCAK–8′35″, tundish (*b*) LCAK, slab (*c*) LCAK, and a rejected slab (*d*) LCAK.

from structural-determined to adhesive-controlled growth. At high supersaturation, VKS growth over-rules BCF growth. The two-dimensional nuclei are preferentially formed at the surface locations with the highest supersaturation gradients, *e.g.*, at corners. This may result in the growth of so-called hopper crystals (Figure 1, right). At very high supersaturation, growth becomes unstable and the crystal corners grow along the supersaturation gradient, which may result in the formation of dendrites. Spherolites are formed at even higher supersaturation, when growth is independent of the crystal-steel interface (isometric growth). Thus, the difference between spherolites and dendrites is defined by the stability of the developing surface during growth. For detailed information on morphological stability, the reader is referred to References 18 through 21.

Rough surfaces do not show flat terraces or clear steps,

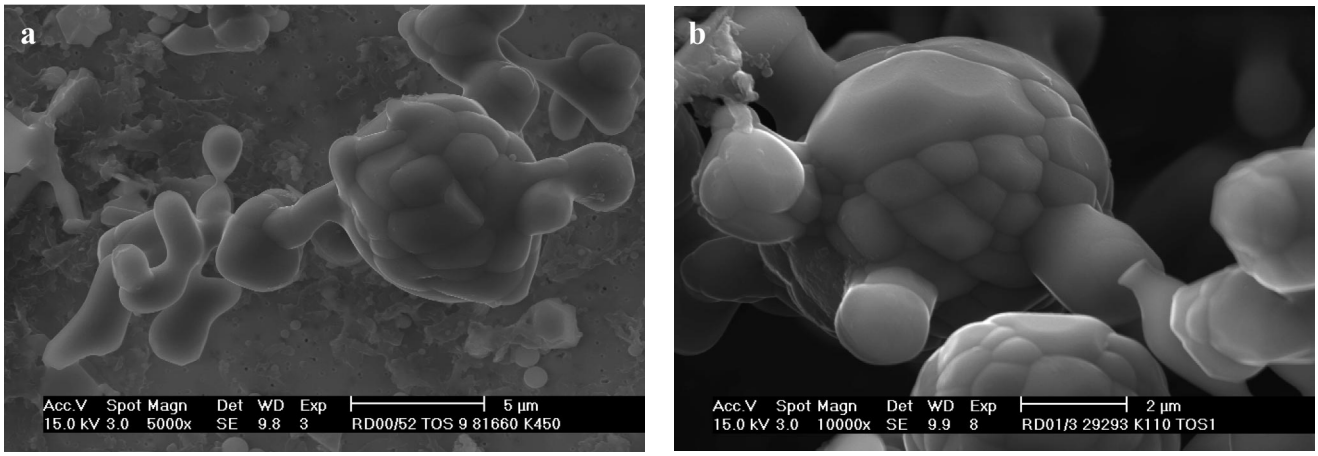

Fig. 6—Ends of dendrite tips frequently consist of apparently agglomerated particles, which form larger and faceted particles due to sintering ((*a*) MCAK–13′21″ and (*b*) LCAK–5′).

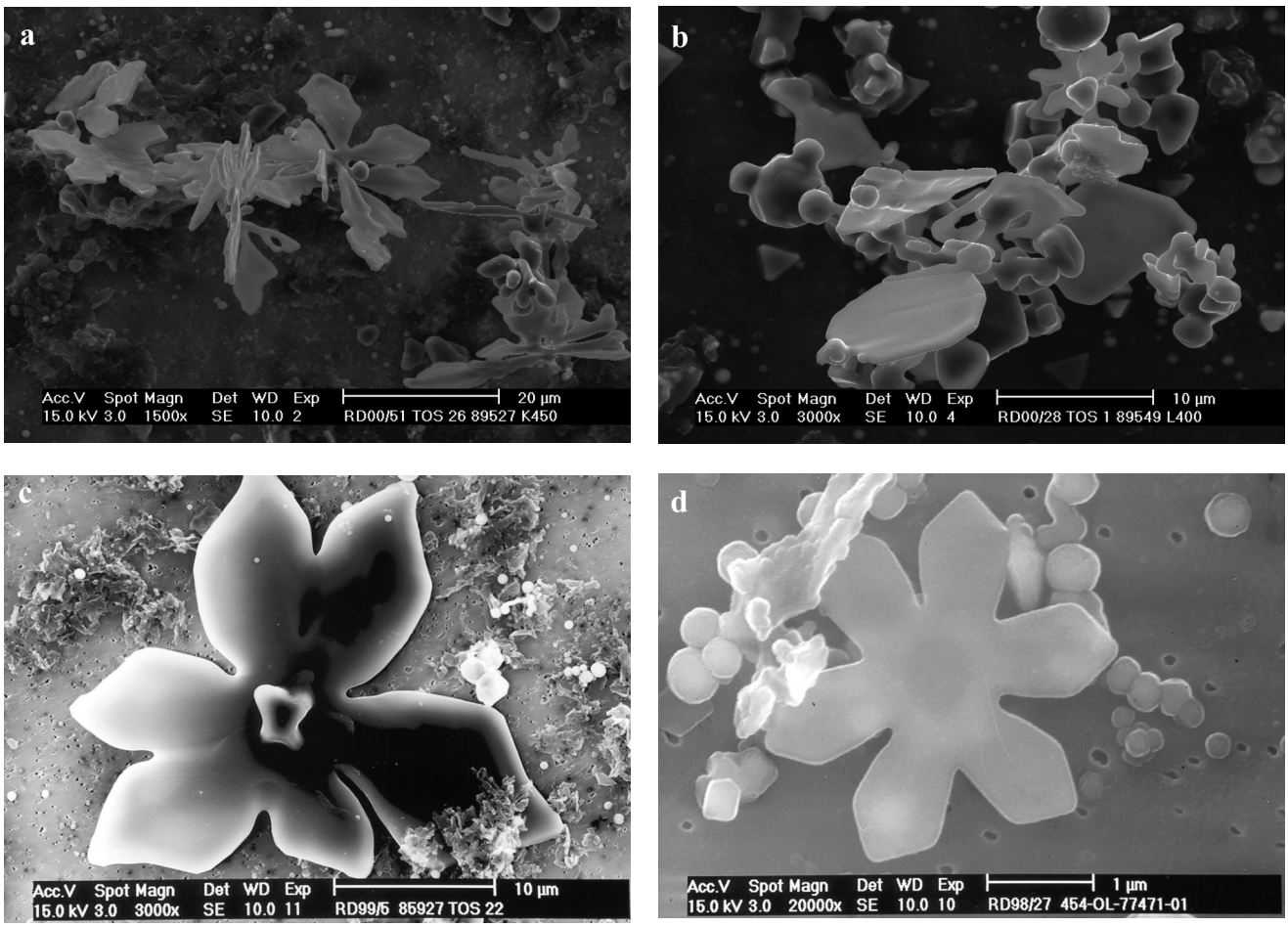

Fig. 7—Platelike inclusions in clusters occur frequently as dendrites. The trigonal symmetry is clearly recognizable ((*a*) MCAK–39′09″, (*b*) LCSAK–2′20″, (*c*) MCAK, 34′44″, and (*d*) LCAK–18′).

and their topology varies in altitude by several growth layers. Roughening due to large adhesive growth is called kinetic roughening, while thermodynamic roughening is due to temperature and the interactions between the surface atoms. In the latter case, the transition from stable to unstable growth occurs at the roughening temperature, at which the entropy of the surface is increased by an average occupation of atom sites. Jackson put forward a general equation to estimate whether a surface is either flat (stable) or rough (unstable):[17]

$$\alpha = \zeta \frac{L}{\mathrm{R}T_m} \qquad [2]$$

where L is the melting enthalpy, T_m the melting temperature,

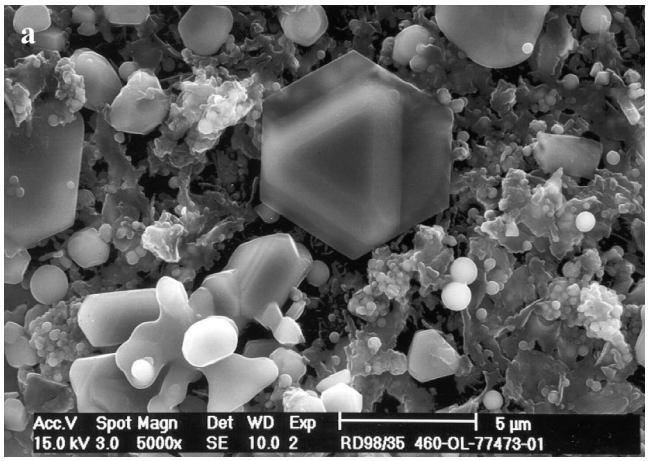

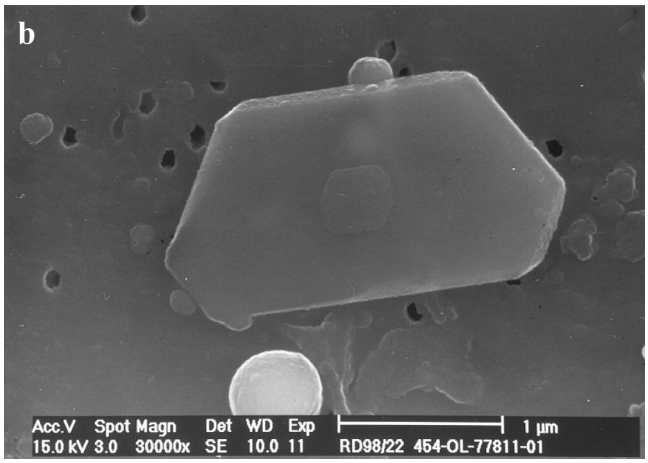

Fig. 8—Singular platelets occur as trigonal or hexagonal plates. Sometimes rhombohedral facets occur ((*a*) LCAK–42′ and (*b*) LCAK–11′).

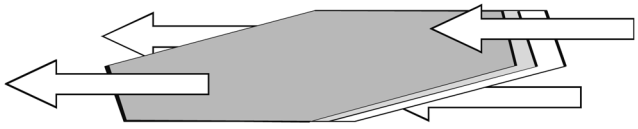

Fig. 9—One-directional supply of components may give rise to growth at one side of the crystal. The arrows indicate the flow direction.

and ξ an orientational factor. Transition from stable to unstable growth occurs for α between 2 and 3. Though steelmaking temperatures are high, thermodynamic roughening does not occur in the case of nonmetallic inclusions in steel, because L is very large, *i.e.*, α is about 7.6.

Sunagawa[17] explains the change from polyhedral, hopper towards dendritic and spherical morphology by considering the different growth mechanisms (Figure 2). Figure 2 is a schematic diagram: different growth mechanisms may occur simultaneously at different parts of a single crystal.

A third parameter that may influence the growth rate and, hence, the morphology of crystals is the presence of impurities adsorbed at the surface. Impurities are species, *e.g.*, atoms, which differ from those in the pure crystalline compound. The influence of these impurities depends on their nature and the sites that they occupy. In particular, during adsorption on terraces, which only occur on flat faces, impurities may hinder the spreading of a growth layer. This pinning effect occurs if the distance between adsorbed impurities is less than twice the size of the critical two-dimensional nucleus. Preferential adsorption of impurities on certain faces may cause significant deviation of the structural-defined habit. An example with respect to steel is sulfur, which may enhance the formation of flake graphite, while magnesium or cerium favors the formation of nodular graphite.[18]

III. SPHERICAL INCLUSIONS

In general, spherical inclusions are considered as being liquid at steelmaking temperatures, which is a very reasonable assumption for manganese silicate and calcium aluminate inclusions, but less so for aluminum oxide. In the present research, three mechanisms for the formation of solid spherical aluminum oxide particles have been found.

(1) Due to the addition of metallic aluminum, manganese silicate inclusions in high-manganese, high-silicon steel grades transform to aluminum oxide.[13] Manganese silicate is liquid at steelmaking temperatures and thus its shape is spherical. Aluminum is a stronger deoxidizer than manganese and silicon, and therefore, it replaces manganese and silicon in the liquid inclusions. The presence of small amounts of silicon or manganese in large aluminum oxide particles substantiates this hypothesis.[13] Apparently, the exchange process does not affect the initial shape of the liquid manganese silicate inclusions. Transformation of prior manganese silicate inclusions is only relevant in silicon-aluminum–killed steels.
(2) Spheroids can result from adhesive growth if supersaturation or thermodynamic roughening is sufficiently high that unstable growth can occur. Once nuclei are formed, they act as sinks with respect to aluminum oxide. Recently, we were able to prove that the small (on average, 0.6 μm) spherical aluminum oxides in TOS samples and in dual samples are formed during sampling of the liquid steel[22] and, therefore, do not represent inclusions present in the liquid steel. Occasionally, spherical inclusions with small facets have been observed (Figure 3b). Formation of facets can be attributed to a decreased level of supersaturation, such that for certain faces, unstable growth changes to layer growth. The presence of concave facets supports this hypothesis.
(3) Coarsening of dendrites was proposed as a source of spherical aluminum oxide particles.[23] During the present research, indications of dendrite coarsening have been observed occasionally (Figure 4). The mechanism implies formation of clusters/dendrites followed by (surface) diffusion of aluminum oxide from the neck toward the thicker parts. Because the process is diffusion-controlled, transition from dendrites into spherical particles is expected to be rather slow.

IV. CLUSTERS AND DENDRITES

Dendrites and clusters are the most frequently reported types of inclusions. Dendrites grow along supersaturation gradients. As a typical example of unstable growth, facets are usually lacking and both dendrite branches and tips are

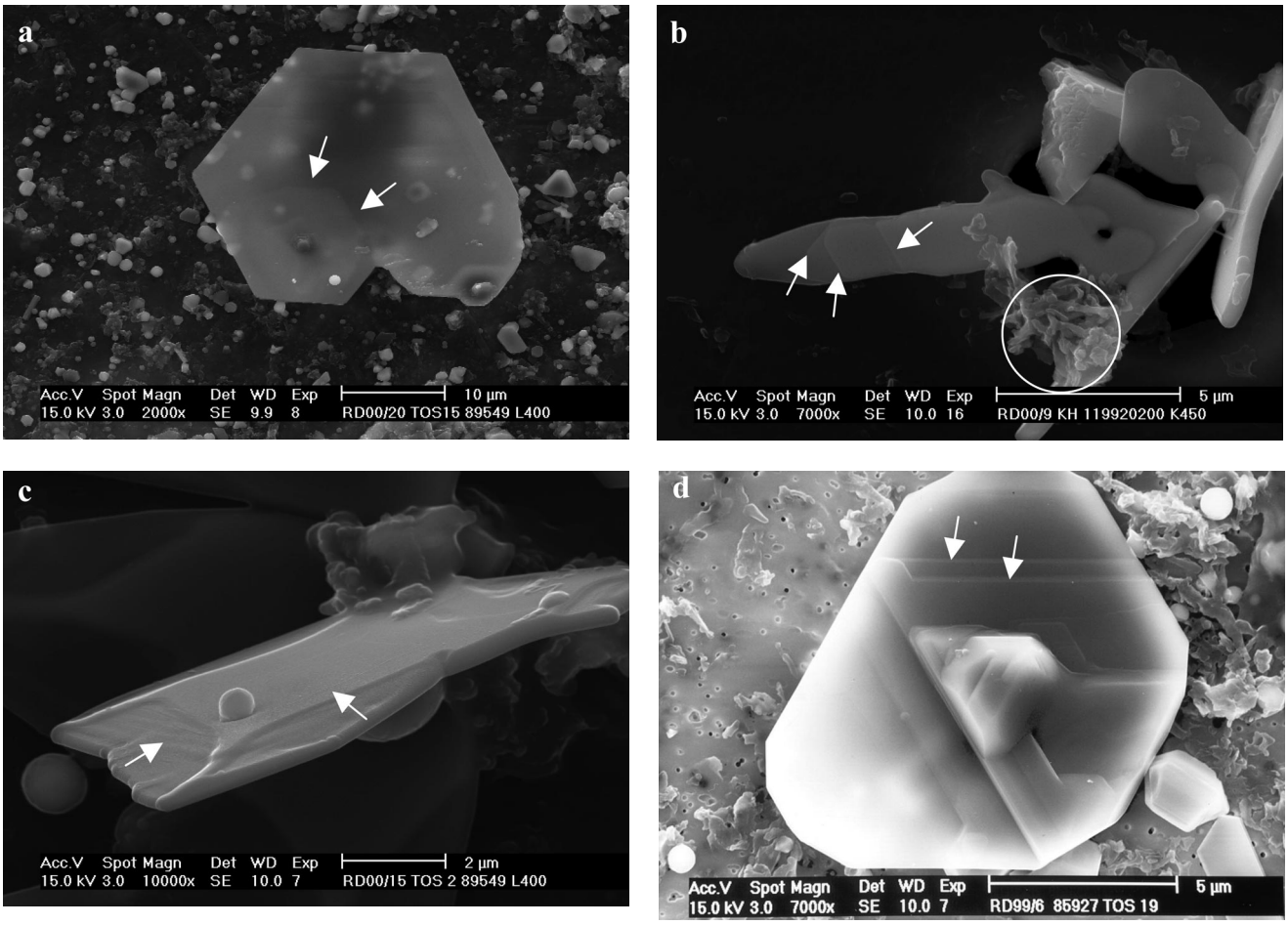

Fig. 10—Macroscopic steps at platelike inclusions. Impurities may hinder the spreading of growth layers ((*a*) LCSAK–26′17″, (*b*) MCAK–slab, (*c*) LCSAK–3′30″, and (*d*) MCAK: 25′01″).

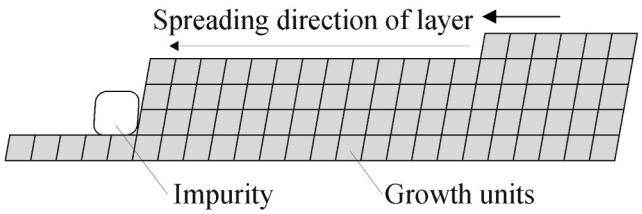

Fig. 11—Schematic drawing of the formation of a macroscopic step due to blockage of an impurity species.

rounded (rough surfaces) (Figure 5). During growth, supersaturation may decrease. As a result, growth rate slows down, and facets are formed (layer growth). This can be seen in Figure 5(c), which shows a dendrite of which the lower part is bounded by rounded surfaces and its tip by facets (the growth direction is indicated by the arrow).

In contrast to dendrites, clusters have an irregular shape, which forms an open network of aluminum oxide. Steinmetz *et al.*[6] explains the random shape of clusters by turbulence in the steel bath during dendritic growth. The difference between dendrites and clusters is determined by the turbulence in the reaction zone. Dendrites show a well-defined growth direction, while in clusters, the *dendrite* may have grown in varying directions dependent on the supersaturation gradients and growth of tips can either stop or become reactivated. The crystal growth mechanism forming dendrites and clusters is similar, but the presence or absence of turbulence gives rise to different shapes. Indeed, cluster formation has been reported on the interface between deoxidized and undeoxidized steel,[5,6] which accounts for high mass transfer (and turbulence) of dissolved oxygen and aluminum along the interface. Transmission electron microscopy proved that clusters consist of monocrystalline corundum with only very slight variation in orientation,[5,6] which is in agreement with growth of a single crystalline particle.

Frequently, cluster tips appear as agglomerates of rounded particles (Figure 6). The rounded shapes have been explained by growth in oxygen-rich steel[6] and by decreased reaction speed (due to lower supersaturation).[24] The agglomerated nature suggests that the rounded shape at the dendrite tip is not the result of growth, but due to densification of the cluster, though capture of singular particles cannot completely be excluded. Initially, the spheres consist of rounded particles, but sintering gives rise to the formation of facets. Sintering accounts for a decrease of the interfacial area. Because of diffusion along the interface, the energetically most favorable surface/interface configuration is created, *i.e.*, a smooth facet with minimum surface energy. Thus, a cluster may change morphology after its primarily formation due to sintering.

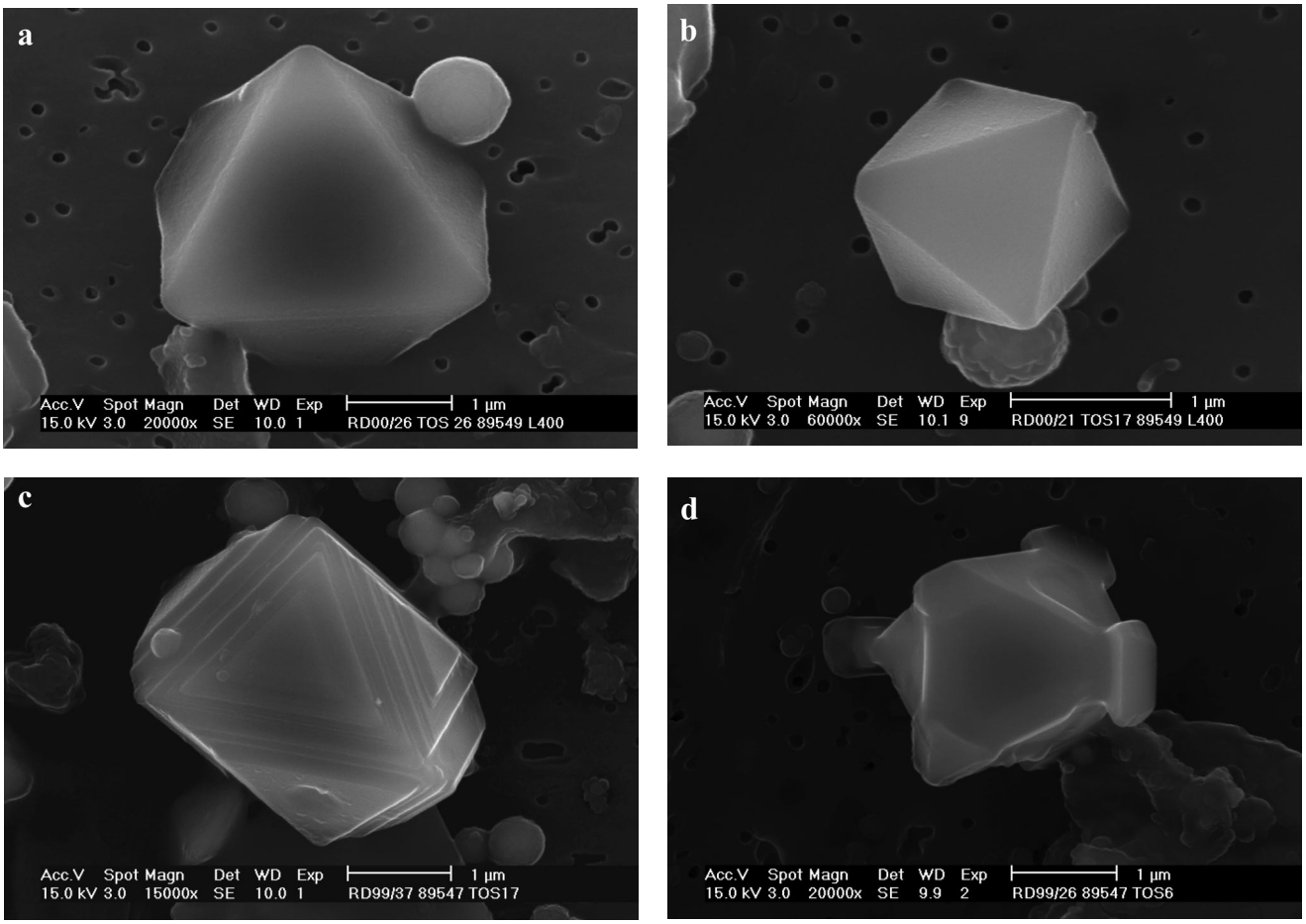

Fig. 12—Octahedral inclusions exhibit flat faces ((*a*) LCSAK–44′20″), concave faces ((*b*) LCSAK–28′45″), convex-stepped faces ((*c*) LCSAK–28′56″), or a hopper morphology ((*d*) LCSAK–7′16″).

V. PLATELIKE INCLUSIONS

Platelike inclusions are characterized by their platy character, which accounts for a large surface-to-volume ratio. In the open network of clusters, platelike inclusions occur frequently with corners that developed far into the melt (Figure 7). The particles have grown dendritically, while retaining their platelike character. Their trigonal symmetry can be recognized in Figure 7. The tips can be faceted (smooth surface) or rounded (rough surface); the platelike shape, however, is not affected. This indicates that the transition from layer growth to unstable growth occurs easier on the rhombohedral faces than on the platy {111} face.

Individual platelike inclusions occur mostly as trigonal or hexagonal platelets (Figure 8). In some cases, plates are elongated, which is assumed to be the result of growth along convection streams, *i.e.*, one-directional supply of components (Figure 9).

The trigonal symmetry of the platelike inclusions suggests that the corresponding aluminum oxide structure is corundum (and certainly not γ-, δ-, or θ-Al_2O_3). Based on this structure, a rhombohedral habit is expected,[25,26,27] but corundum is frequently reported as platelets. The platy {111} habit differs from the structurally defined habit. The following discussion explains why the relative growth rate of the {111} face decreases.

Sunagawa[17] investigated the surface topologies of the {111} face and found that the step separation is much larger in the case of vapor growth than in the case of solution growth. Since rhombohedral morphologies appear when crystals grow from hydrous solution, whereas a thin platelike habit occurs in growth from a vapor, Sunagawa assumes higher adsorption rates of growth units in the case of solution growth.

Commonly, oxygen atoms and a small number of interstitial cations cover the surface of oxide compounds. However, aluminum atoms cover the platy {111} face of corundum. Thus, the {111} face of corundum differs from the other corundum faces and, therefore, its growth rate may be influenced in a different way by supersaturation or the presence of impurities. Habit changes of corundum are usually discussed with respect to growth at different temperatures or different growth media (vapor, solution, or melt). Hartman[25] concludes that the platelike habit can be understood by considering adsorption of impurities on the {111} face. The impurity hypothesis does not necessarily exclude a structural influence. If the concentration of screw dislocations is significantly less on the {111} face than on the other faces, impurities will more dramatically affect its growth rate.

The thin platelets have a high surface-to-volume ratio, which is also an indication that external factors affect the

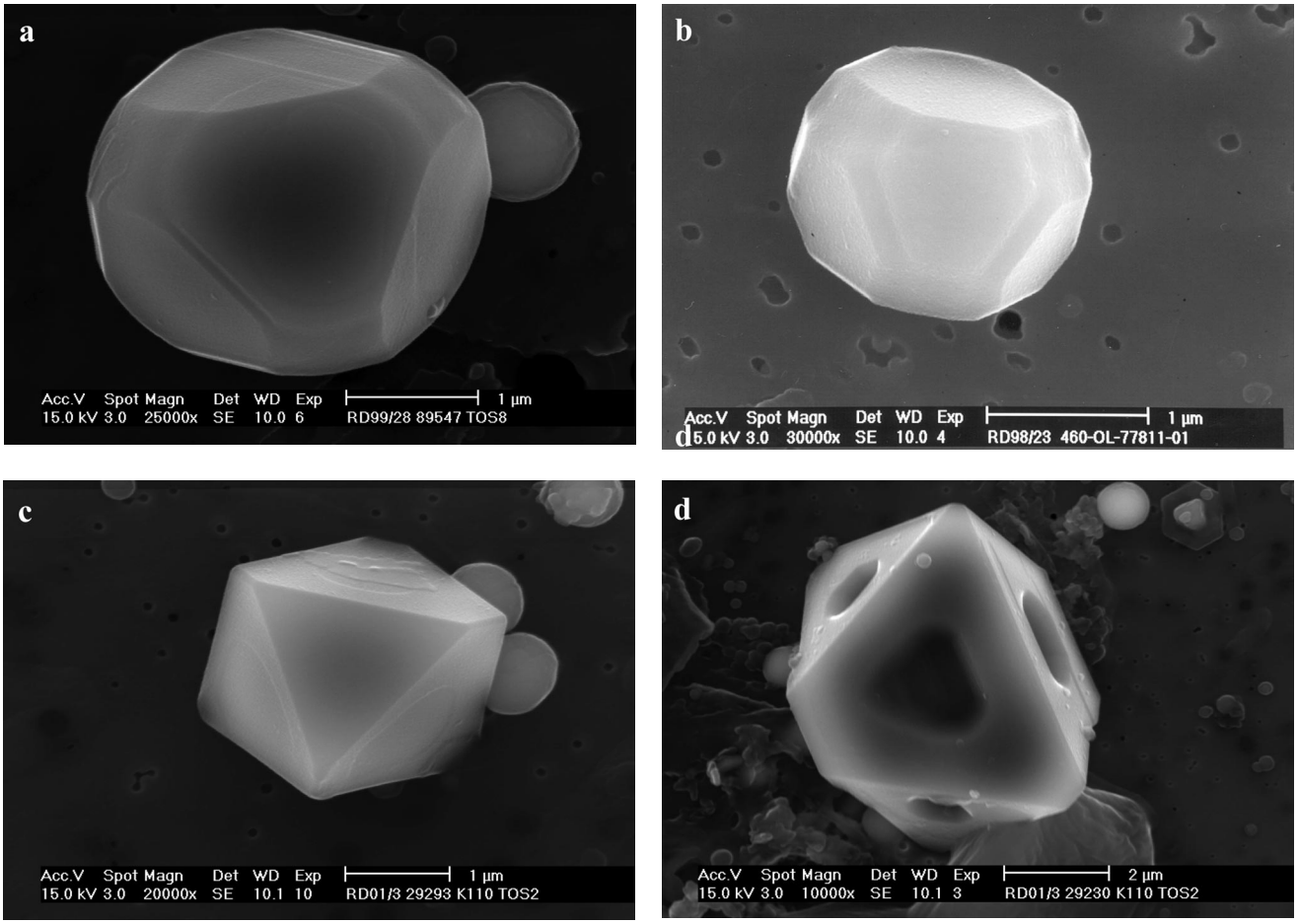

Fig. 13—Non octahedral inclusions show mostly trigonal symmetry ((*a*) LCSAK–10′28″, (*b*) LCAK–27′, and (*c*) and (*d*) LCAK–10′).

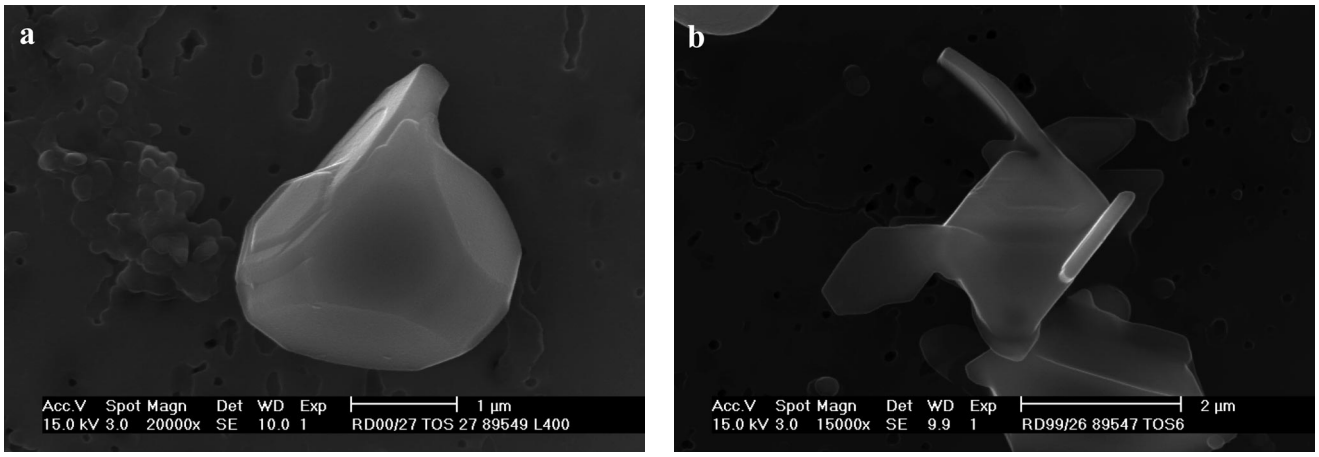

Fig. 14—Platelike overgrowth onto existing particles ((*a*) LCSAK–45′50″ and (*b*) LCSAK–7′16″).

morphology. Some {111} surfaces exhibit macroscopic islands or steps (Figure 10). This supports the hypothesis that impurities play a major role. Steps are expected to spread fast over the surface, and macroscopic steps are explained by the pinning effect of impurities (Figure 11). The platelike dendrite in Figure 10(b) exhibits a rough shape with straight steps, which is an indication that the growth conditions have changed.

VI. POLYHEDRAL INCLUSIONS

Two main types of polyhedral inclusions are recognized in the present research, *i.e.*, octahedra, and nonoctahedra. The

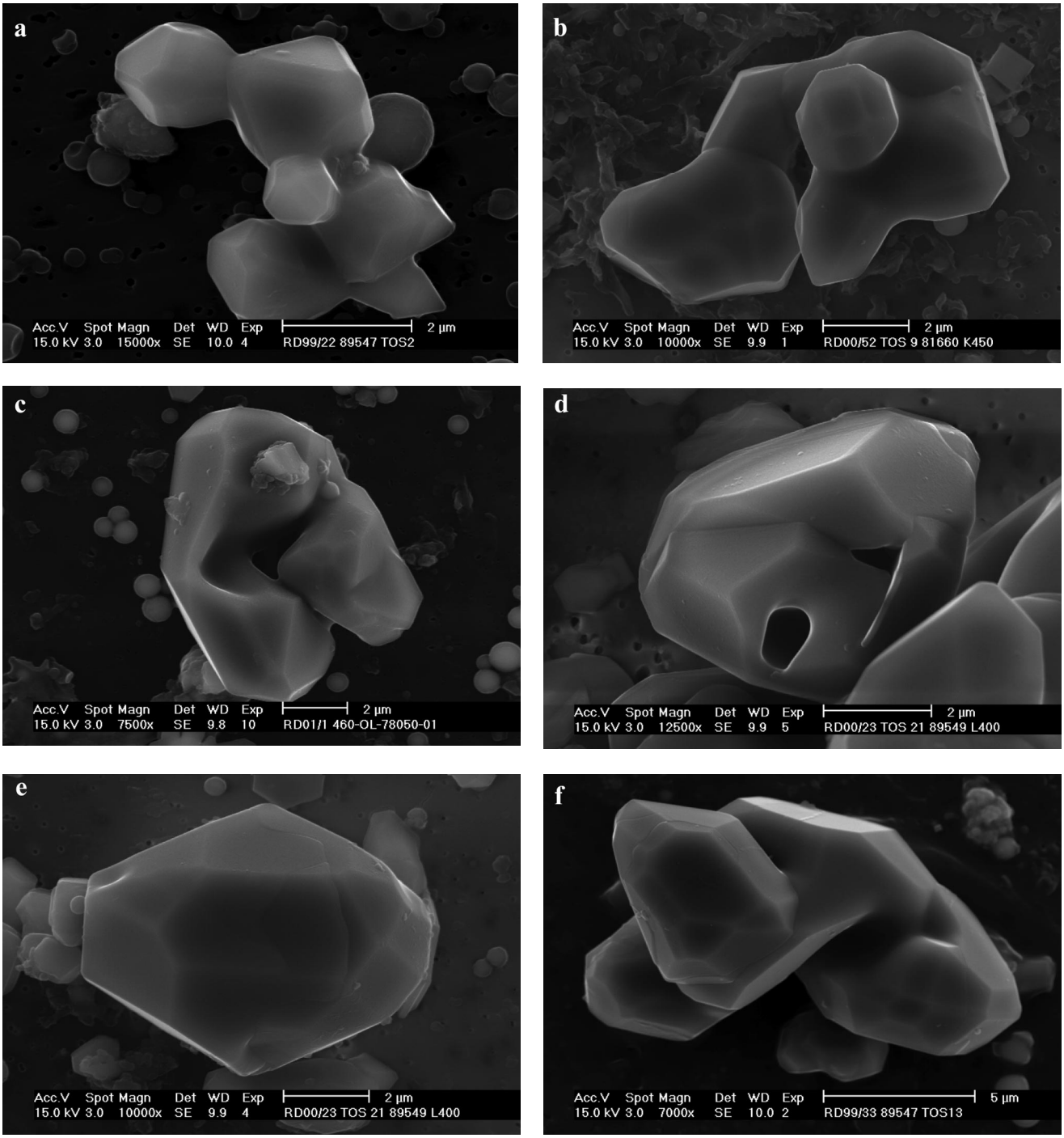

Fig. 15—Aggregation of small polyhedral particles may lead to the formation of large aggregates and, after sintering, to large polyhedra ((*a*) LCSAK–0′46″, (*b*) MCAK–9′20″, (*c*) LCAK–38′, (*d*) and (*e*) LCSAK–36′20″, and (*f*) LCSAK–18′41″).

octahedra exhibit flat faces, concave faces, convex-stepped faces, or hopper morphology (Figure 12). The convex-stepped habit is probably due to impurities, while the flat faces, concave faces, and hopper morphology can be understood in terms of increasing supersaturation.

Examples of nonoctahedral inclusions are shown in Figure 13. Nonoctahedral inclusions mostly are trigonal or hexagonal prisms, or rhombohedra, though less well-defined shapes occur as well. Figure 13(a) looks very similar to the spherical inclusions with small facets (compare with Figure 3). Figure 13(d) is hopperlike crystal.

The presence of both octahedral-type and trigonal habits indicates that, apparently, more than one type of aluminum oxide is present in steel. Apart from corundum, metastable aluminum oxides such as γ-, δ-, and θ-Al_2O_3 have been reported in steel on the basis of X-ray diffraction measurements.[28,29] Exchange of manganese or iron from oxide inclusions by aluminum dissolved in the steel has been proposed as a possible mechanism for the formation of metastable aluminum oxides.[30]

Some inclusion morphologies may be understood by considering overgrowth of corundum onto octahedral faces, *e.g.*,

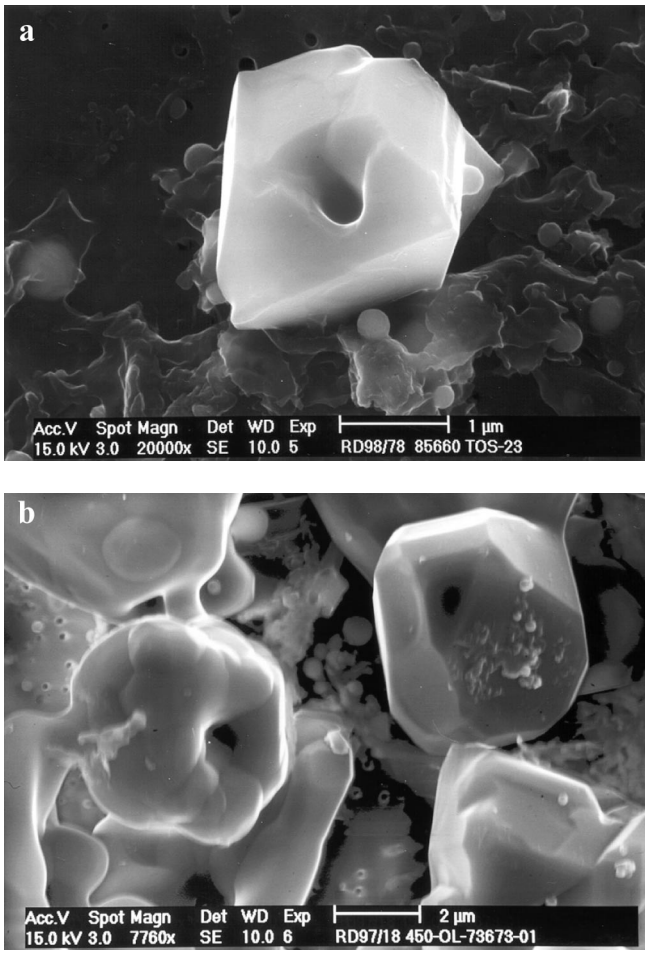

Fig. 16—Small inclusions may originate from aggregated articles ((*a*) MCAK–24′21″ and (*b*) LCAK–3′ after semikilling to about 400 ppm).

plates that are overlying octahedral faces and extend into the steel (Figure 14). The octahedral faces probably act as preferred sites for epitaxial overgrowth of corundum, because only a slight lattice misfit between the two phases exists, *i.e.*, (111) face of hexagonal close-packed structure onto {111} face of cubic closed-packed structure.[31] Similar to plate-like inclusions, we assume that the platelike habit of the overgrown phase is caused by the influence of impurities. Based on our observations, we are not able to tell whether the overgrowth occurs at a certain moment of primary growth or whether it is due to reoxidation (secondary growth).

VII. ACCRETIONAL GROWTH

Growth by accretion of particles is well known.[32] Initially, aggregates consist of individually recognizable polyhedral inclusions, but with increasing ladle metallurgy treatment time, they become more compact due to sintering (Figures 15(a) through (e)). Intensive sintering may cause pore formation in particles (Figure 15(d)). Though sintering implies densification of the aggregates, their average sizes increase with holding time.[13] Therefore, after the initial growth of inclusions due to the addition aluminum, and after the removal of clusters from the steel bath, agglomeration is expected to play a major role with respect to the formation of large and detrimental inclusions (Figure 15(f)).

Not only large inclusions, but also small particles, may have a polycrystalline origin (Figure 16). Thus, small polyhedral particles may have developed from a single either homogeneous or heterogeneous nucleus or by simultaneous growth and accretion of particles. The actual mechanism depends on the concentration of the oxide particles, *i.e.*, their probability to meet and attach.

VIII. CONCLUSIONS

The morphology of an inclusion depends on the following factors.

1. *Its atomic structure*: Liquid inclusions are always spherical, because of the smallest surface-to-volume ratio. In the case of a crystalline inclusion, the relative growth rate or the relative surface energies of the facets define the inclusion form.
2. *The degree of supersaturation*: Determines whether an inclusion shows facets or whether its shape deviates from the thermodynamic- (structure-) determined form. At high supersaturation, *e.g.*, during sampling (fast cooling and solidification), unstable but isometric growth leads to the formation of spherical aluminum oxides. In industrial melts, the addition of aluminum gives rise to high supersaturation of oxygen and aluminum. The fast formation and growth of aluminum oxide inclusions results in morphological instability of their surface. Therefore, the aluminum additions for deoxidation of the steel give rise to the formation of dendrites and clusters. Turbulence of the reaction zone favors the formation of clusters. Moreover, agglomeration of dendrites and clusters, *e.g.*, as result of convection flow or different emerging velocities, may account for very large networks of aluminum oxide (Figure 5(d)). Just after aluminum addition, the concentration of aluminum in the steel will not be homogeneous. Therefore, also, the degree of supersaturation is not homogeneous throughout the ladle. At locations of relative low supersaturation, small (less than 5 μm) faceted inclusions are formed. If inclusions are already present in the steel before the addition of aluminum, *e.g.*, manganese silicate, these particles are transformed into aluminum oxide.
3. *The presence of impurities*: Impurities may influence the growth of specific facets and in such affect the inclusion form.
4. *Agglomeration followed by sintering*: Because of the nonwetting properties of aluminum oxide, attachment always occurs when particles meet. Sintering results in a decrease in interfacial area. Furthermore, rearrangement of the surface or the bulk structure during sintering may give rise to a lower specific interfacial energy.

ACKNOWLEDGMENTS

This research has been funded by IWT-SIDMAR-MTM Project No. 99-0251. The authors thank C.F. Woensdregt (University Utrecht) for his critical reading of the manuscript and his constructive suggestions.

REFERENCES

1. H. Straube, G. Kühnelt, and E. Plöckinger: *Arch. Eisenhüttenwes.*, 1967, vol. 38 (7), pp. 509-18.
2. L. Luyckx: *J. Met.*, 1968, vol. 6, pp. 61-8.
3. G. Konig and T. Ernst: *Radex-Rundschau*, 1970, vol. 2, pp. 67-98.

4. E. Steinmetz and H.-U. Lindenberg: *Arch. Eisenhüttenwes.*, 1976, vol. 47 (4), pp. 199-204.
5. E. Steinmetz, H.-U. Lindenberg, W. Mörsdorf, and P. Hammerschmid: *Arch. Eisenhüttenwes.*, 1977, vol. 48 (11), pp. 569-74.
6. E. Steinmetz, H.-U. Lindenberg, W. Mörsdorf, and P. Hammerschmid: *Stahl Eisen*, 1977, vol. 97 (23), pp. 1154-59.
7. A.S. Venkatadri: *Trans. Iron Steel Inst. Jpn.*, 1978, vol. 18, pp. 591- 600.
8. T.B. Braun, J.F. Elliottand, and M.C. Flemings: *Metall. Trans. B*, 1979, vol. 10B, pp. 171-84.
9. S.W. Robinson, I.W. Martin, and F.B. Pickering: *Met. Technol.*, 1979, pp. 157-69.
10. H. Fedriksson and Ö. Hammar: *Metall. Trans. B*, 1980, vol. 11B pp. 383-408.
11. E. Steinmetz, H.-U. Lindenberg, W. Mörsdorf, and P. Hammerschmid: *Stahl Eisen.*, 1983, vol. 103 (11), pp. 539-45.
12. E. Steinmetz and C. Andreae: *Steel Res.*, 1991, vol. 62 (2), pp. 54-59.
13. R. Dekkers, B. Blanpain, P. Wollants, F. Haers, C. Vercruyssen, and B. Gommers: Katholieke Universiteit Leuven–Sidmar, Leuven, Belgium, unpublished research, 2001.
14. R. Dekkers, B. Blanpain, P. Wollants, F. Haers, C. Vercruyssen, and L. Peeters: *Proc. 5th Int. Conf. "Progress in Analytical Chemistry in the Steel and Metals Industries*," Luxembourg, May 12–14, 1998, R. Tomellini, ed., Office for Official Publications of the European Communities, Luxembourg, 1999, pp. 610-15.
15. R. Dekkers, B. Blanpain, P. Wollants, F. Haers, C. Vercruyssen, and L. Peeters: *Proc. Extraction and Processing Division of the Minerals, Metals and Materials Society*, San Diego, CA, Feb. 1999, Metals and Materials Society, PA, 1999, pp. 269-77.
16. P. Hartman: *Crystal Growth: An Introduction*, P. Hartman, ed., North-Holland Publ., Amsterdam, 1973, pp. 367-402.
17. I. Sunagawa: *Morphology of Crystals*, Part B, I. Sunagawa, ed., Terra Scientific Publishing, Tokyo, and D. Riedel Publishing, Dordrecht, 1987, pp. 509-87.
18. W. Kurz and D.J. Fisher: *Fundamentals of Solidification*, 3rd ed, Trans Tech Publishing, Aedermannsdorf, Switzerland, 1989, pp. 21-92.
19. R.F. Sekerka: *Crystal Growth: an Introduction*, P. Hartman, ed., North-Holland Publ. Amsterdam, 1973, pp. 403-43.
20. T. Kuroda, T. Irisawa, and A. Ookawa: *Morphology of Crystals*, Part B, I. Sunagawa, ed., Terra Scientific Publishing, Tokyo, and D. Riedel Publishing, Dordrecht, 1987, pp. 590-612.
21. H. Müller-Krumbhaar: *Morphology of Crystals*, Part B, I. Sunagawa, ed., Terra Scientific Publishing, Tokyo, and D. Riedel Publishing, Dordrecht, 1987, pp. 613-43.
22. R. Dekkers, B. Blanpain, P. Wollants, F. Haers, C. Vercruyssen, and B. Gommers: Katholieke Universiteit Leuven–Sidmar, Leuven, Belgium, unpublished research, 2002.
23. M.C. Flemings: *Metall. Trans.*, 1974, vol. 5, pp. 2121-34.
24. W. Tiekink, J. Brockhoff, and J. van der Stel: *Proc. 4th Int. Conf. on Clean Steel*, Balatonszeplak, Hungary, 8–10 June 1992, The Institute of Materials, London, 1992, pp. 704-17.
25. P. Hartman: *J. Cryst. Growth*, 1980, vol. 49, pp. 166-70.
26. W.C. Mackrodt: *Phys. Chem. Minerals*, 1988, vol. 15, pp. 228-37.
27. R. Dekkers, C.F. Woensdregt, and P. Wollants: *J. Non-Crystalline Solids*, 2001, vol. 282, pp. 49-60.
28. A. Adachi, N. Iwamoto, and M. Ueda: *Trans. Iron Steel Inst. Jpn.*, 1966, vol. 6, pp. 24-30.
29. R.G. Smerko and D.A. Flinchbaugh: *J. Met.*, 1968, vol. 20 (7), pp. 43-51.
30. R. Dekkers, B. Blanpain, P. Wollants, F. Haers, C. Vercruyssen, and B. Gommers: *2nd Int. Cong. in the Science & Technology of Steelmaking*, Swansea, United Kingdom, Apr. 10–11, 2001, The Institute of Materials, London, 2001, pp. 655-65.
31. D.R. Clarke: *Phys. Status Solidi A*, 1998, vol. 166 (1), pp. 183-96.
32. U. Lindborg and K. Torssell: *Trans. TMS-AIME*, 1968, vol. 242 (1), pp. 94-102.